Figures and figure supplements

Dissection of zebrafish *shha* function using site-specific targeting with a Cre-dependent genetic switch

Kotaro Sugimoto *et al*

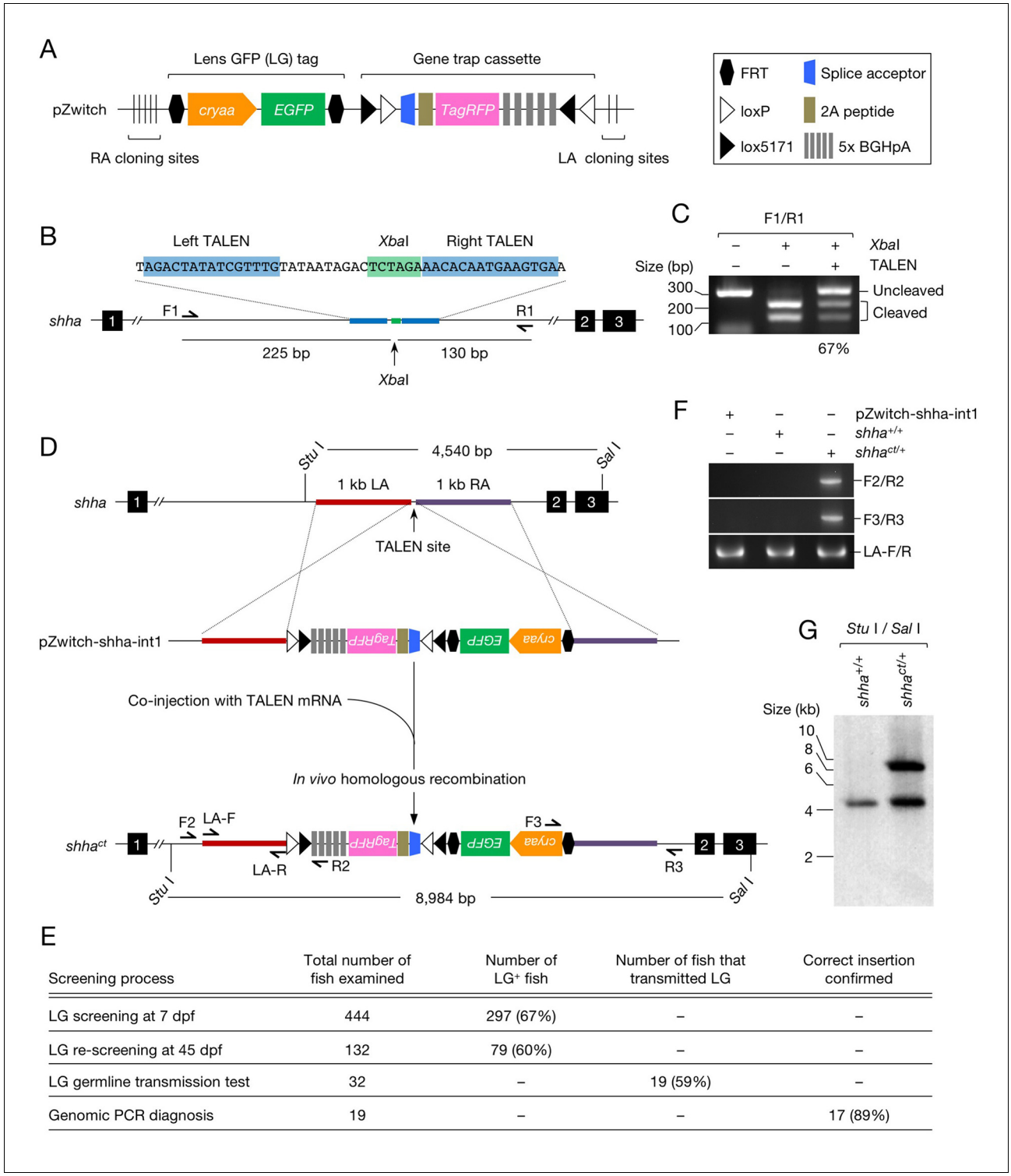

Screening process	Total number of fish examined	Number of LG⁺ fish	Number of fish that transmitted LG	Correct insertion confirmed
LG screening at 7 dpf	444	297 (67%)	–	–
LG re-screening at 45 dpf	132	79 (60%)	–	–
LG germline transmission test	32	–	19 (59%)	–
Genomic PCR diagnosis	19	–	–	17 (89%)

Figure 1. Generation of the *shha* conditional allele using *Zwitch*. (**A**) Schematic of *Zwitch*. (**B**) Schematic of the zebrafish *shha* locus and TALEN used to induce DNA DSBs in intron 1. Exons are indicated by filled boxes with numbers. The binding sites for the TALEN pair are highlighted in blue, and the *Xba*I site in the spacer region is highlighted in green. (**C**) The efficiency of the TALENs in introducing DSBs. *Xba*I digestion of PCR products amplified from the genomic DNA of embryos injected with TALEN mRNAs. The efficiency of the TALEN pair in inducing DSBs (67%) was quantified from the gel image using ImageJ software. (**D**) Schematic of the strategy used to target *shha* via TALEN-mediated homologous recombination with pZwitch-shha-int1. (**E**) The screening process for founders. (**F**) Genomic PCR analysis of the *Zwitch* insertion with the correct orientation. (**G**) Southern blot analysis of the *Zwitch*-modified *shha* allele. BGHpA, bovine growth hormone polyadenylation signal; *cryaa*, α A-crystallin; LA, left arm; RA, right arm.

Figure 1 continued on next page

Figure 1 continued

DOI: 10.7554/eLife.24635.002

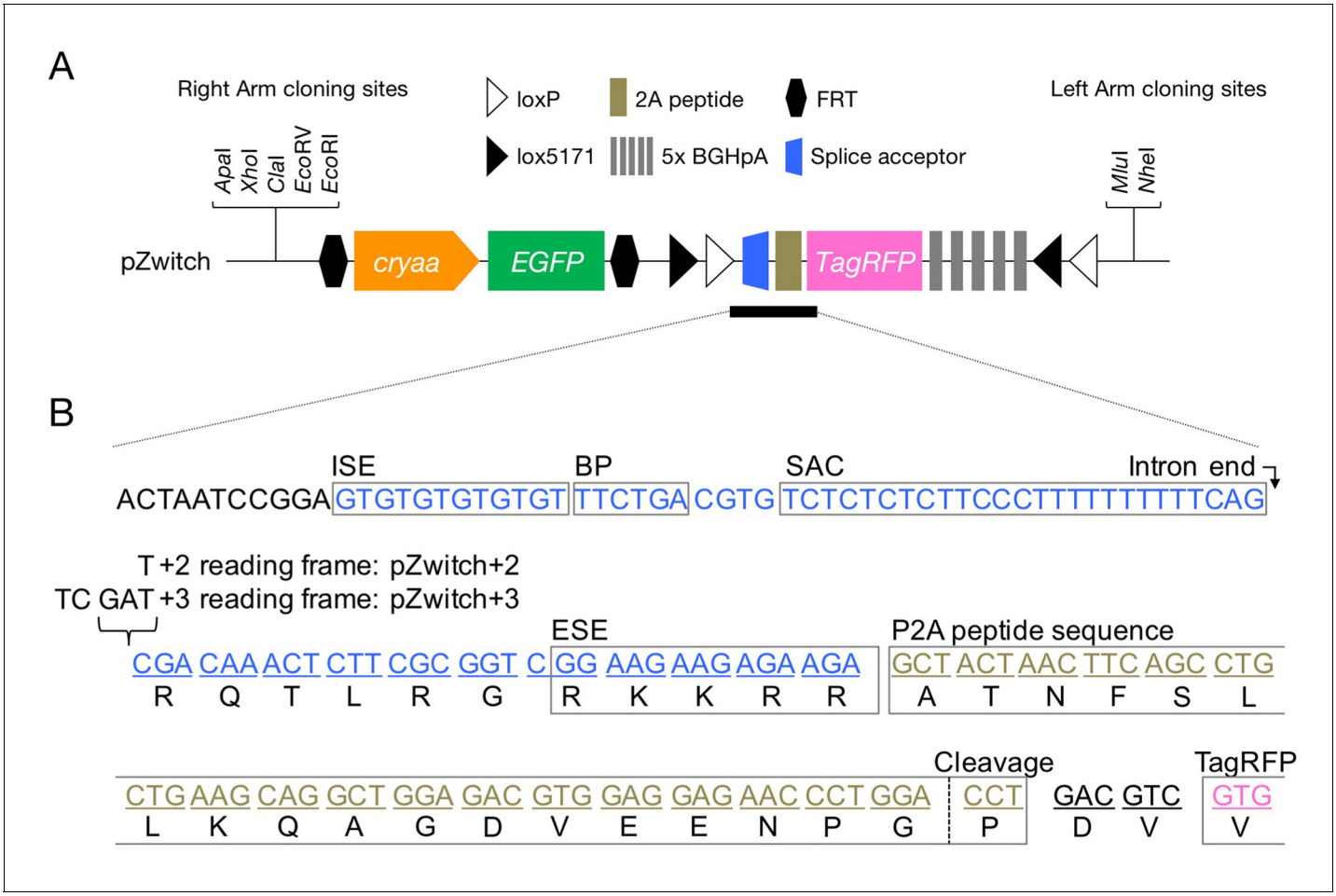

Figure 1—figure supplement 1. pZwitch vector. (**A**) Schematic of pZwitch. (**B**) Sequence of the splice acceptor and P2A components of pZwitch (filled bar in **A**). The splice acceptor sequence was derived from pFT1 (***Ni et al., 2012***). pZwitch for the +2 and+3 reading frames was generated by inserting T and TCGAT, respectively, at the indicated site. BP, branch point; ESE, exonic splice enhancer; ISE, intronic splice enhancer; SAC, splice acceptor consensus.

DOI: 10.7554/eLife.24635.003

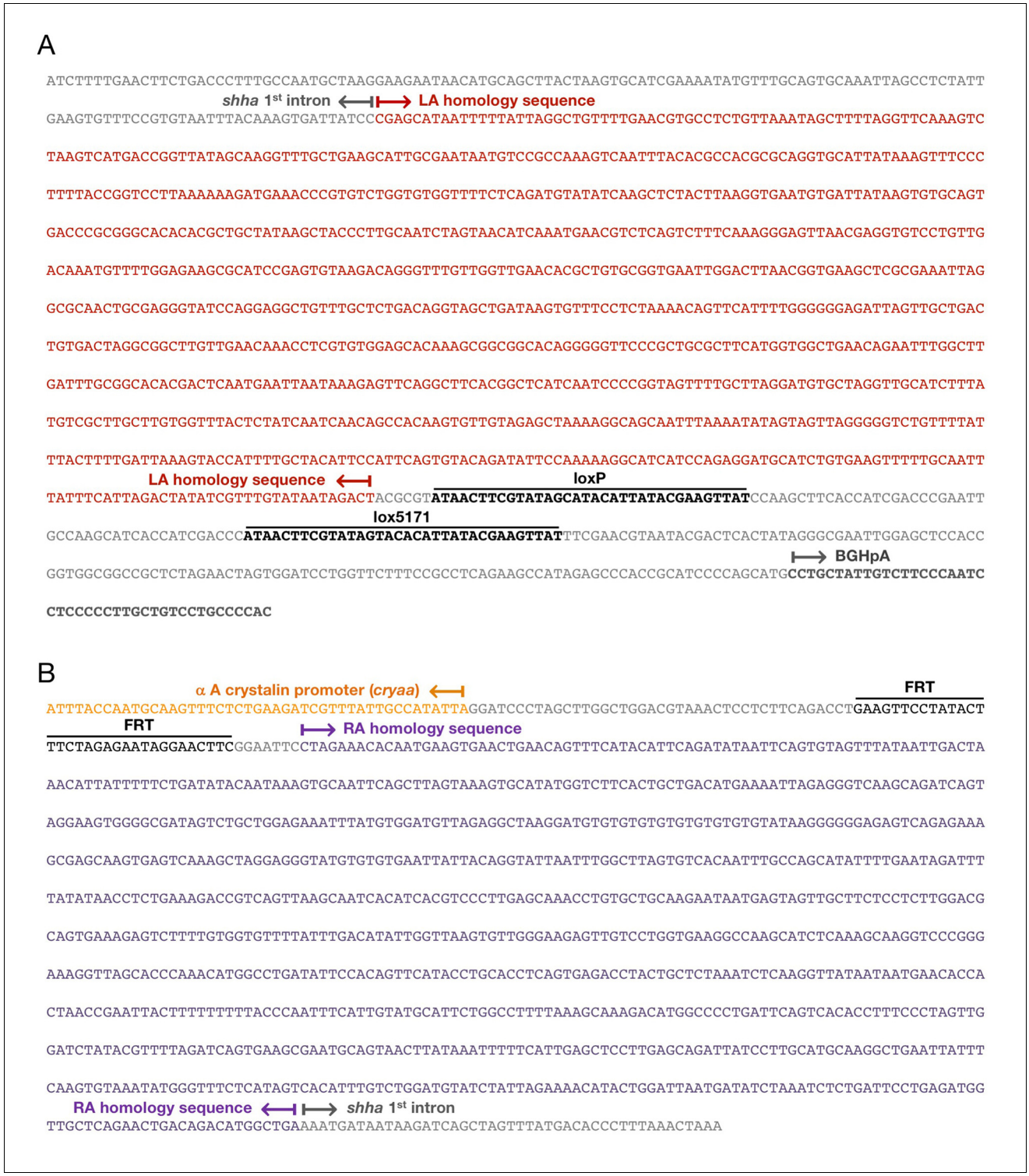

Figure 1—figure supplement 2. DNA sequence of the *shha*^{ct} allele. (**A**) DNA sequence at the 5′ end of the LA homology sequence of pZwitch-shha-int1. (**B**) DNA sequence at the 3′ end of the RA homology sequence of pZwitch-shha-int1.
DOI: 10.7554/eLife.24635.004

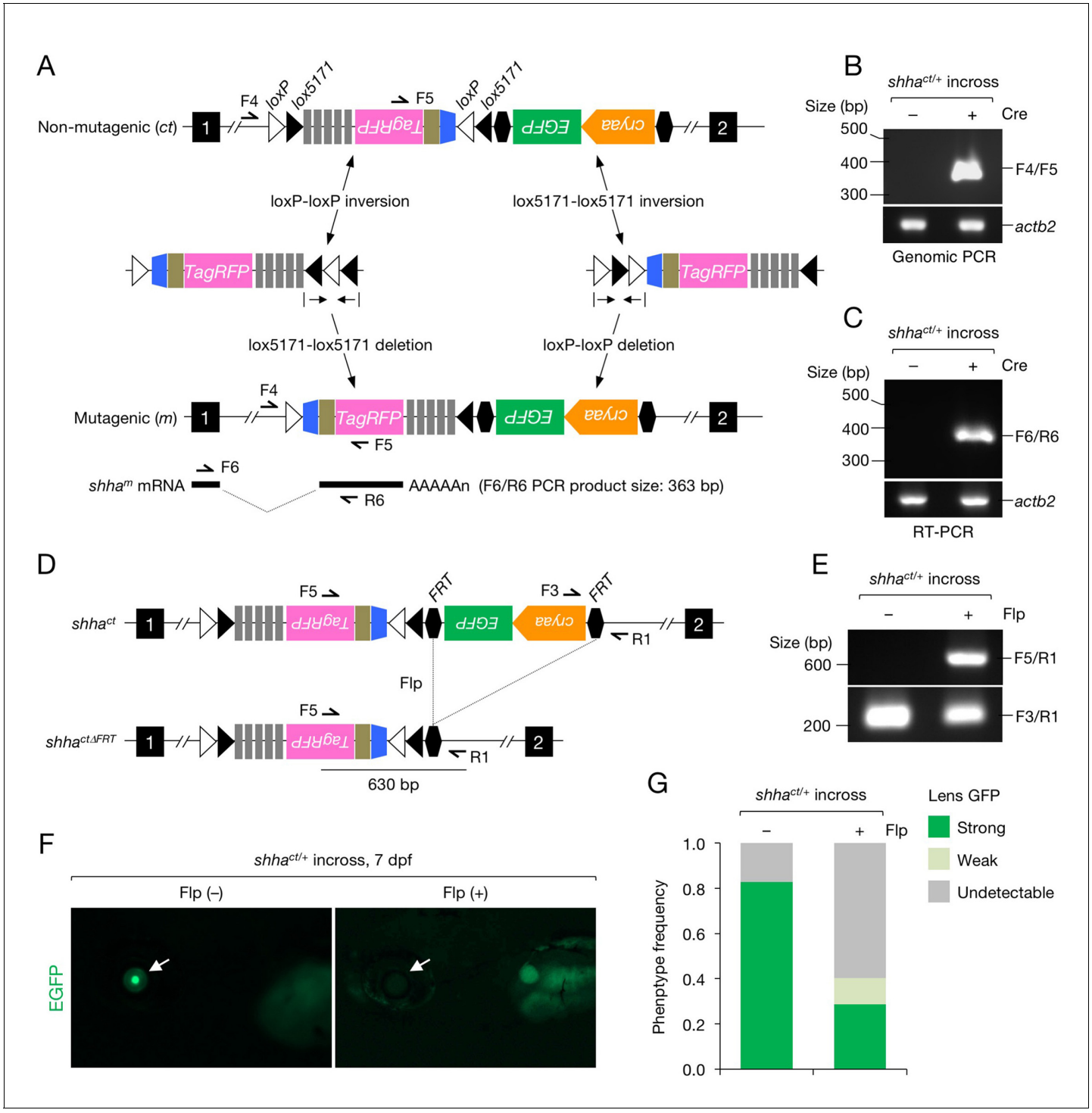

Figure 2. Characterization of the *shha*^{ct} allele. (**A**) Schematic of Cre-dependent conversion of *Zwitch* from the non-mutagenic orientation to the mutagenic orientation. Cre activation induces an inversion between loxP or lox5171 sites and the subsequent excision of loxP or lox5171-flanking DNA sequences (***Schnütgen and Ghyselinck, 2007***), thereby permanently converting *Zwitch* into the mutagenic form and inducing aberrant *shha* splicing. (**B**) PCR analysis of the *Zwitch* inversion. Genomic DNA from 72 hpf Cre^{+} and Cre^{-} *shha*$^{ct/+}$ embryos was analyzed using PCR. (**C**) RT-PCR analysis of *shha* expression in 72 hpf Cre^{+} and Cre^{-} *shha*$^{ct/+}$ embryos. (**D**) Schematic of Flp-mediated excision of the FRT-flanked LG tag in the *shha*^{ct} allele. (**E**) Genomic PCR analysis of Flp-injected (+) or uninjected (–) embryos from a cross of *shha*$^{ct/+}$ adults. PCR using F3 and R1 primers detected *shha*^{ct} alleles in both samples. Flp mRNA was synthesized from linearized pCS2-FLPo (Materials and methods). (**F**) Representative image of embryos injected with Flp mRNA. Arrows indicate the lens. (**G**) Quantification of phenotypes of the embryos analyzed in **F**. A total of 87 Flp-injected (+) and 99 uninjected embryos (–) were analyzed (****$p<1.0 \times 10^{-8}$ Fisher's exact test). dpf, days post-fertilization.

Figure 2 continued on next page

Figure 2 continued

DOI: 10.7554/eLife.24635.005

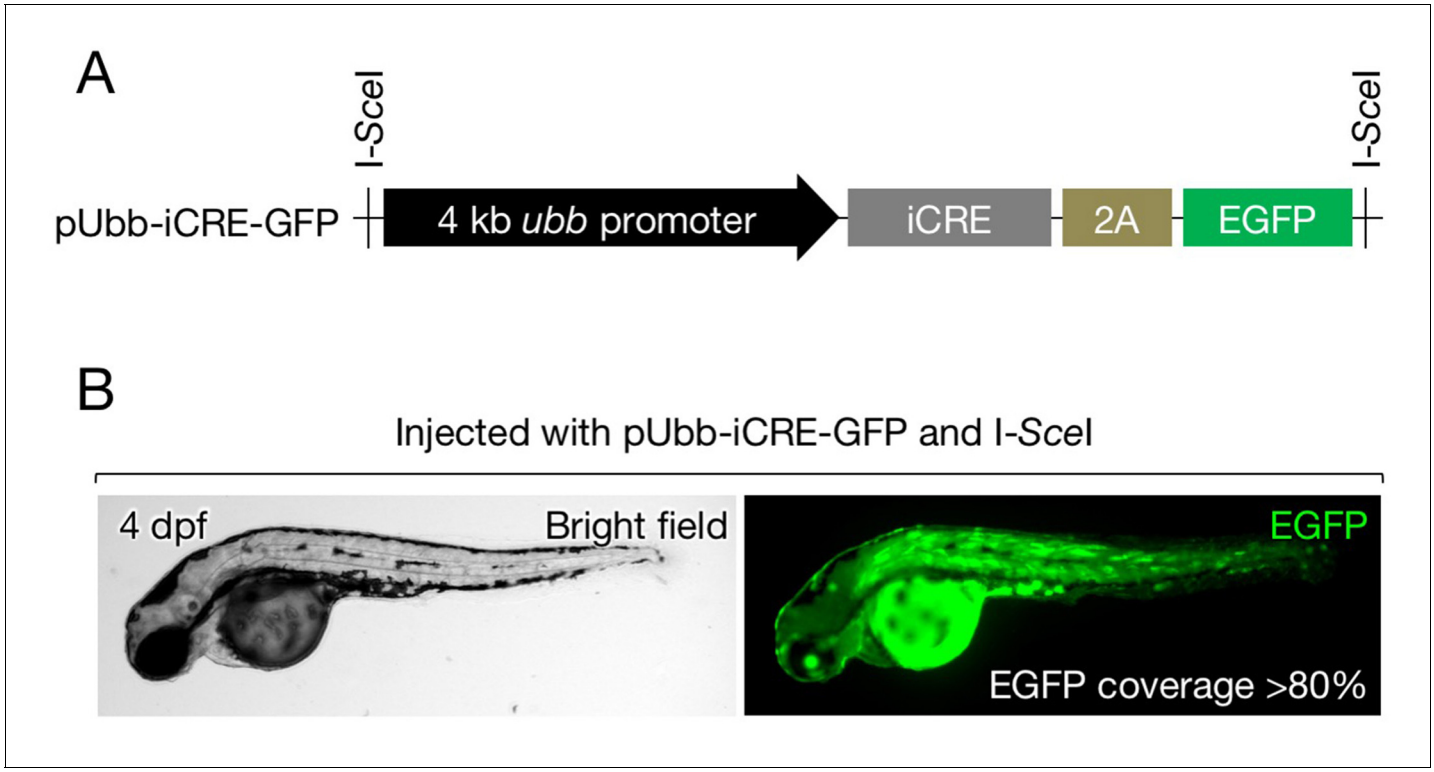

Figure 2—figure supplement 1. Cre expression vector. (**A**) Schematic of pUbb-iCRE-GFP. (**B**) A representative image of embryos injected with pUbb-iCRE-GFP expressing EGFP (right) on approximately 80% of the body surface (left). Embryos expressing EGFP at similar or greater levels were selected for the analysis presented in ***Figure 3A–C***.

DOI: 10.7554/eLife.24635.006

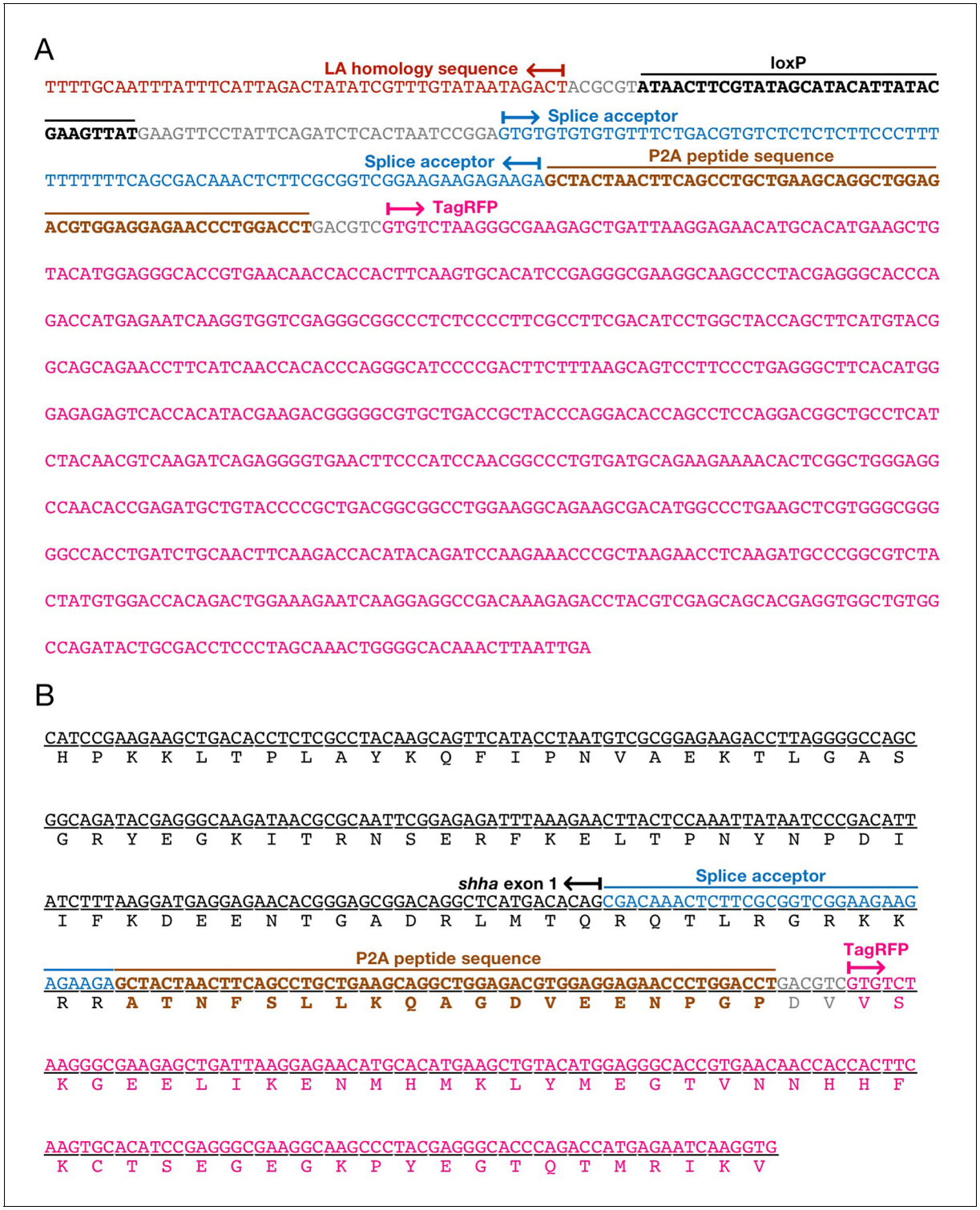

Figure 2—figure supplement 2. DNA sequence of the inverted *shha*^{ct} allele and its transcript. (**A**) DNA sequence of the inverted *shha*^{ct} allele. (**B**) DNA sequence of *shha-P2A-TagRFP* mRNA.

DOI: 10.7554/eLife.24635.007

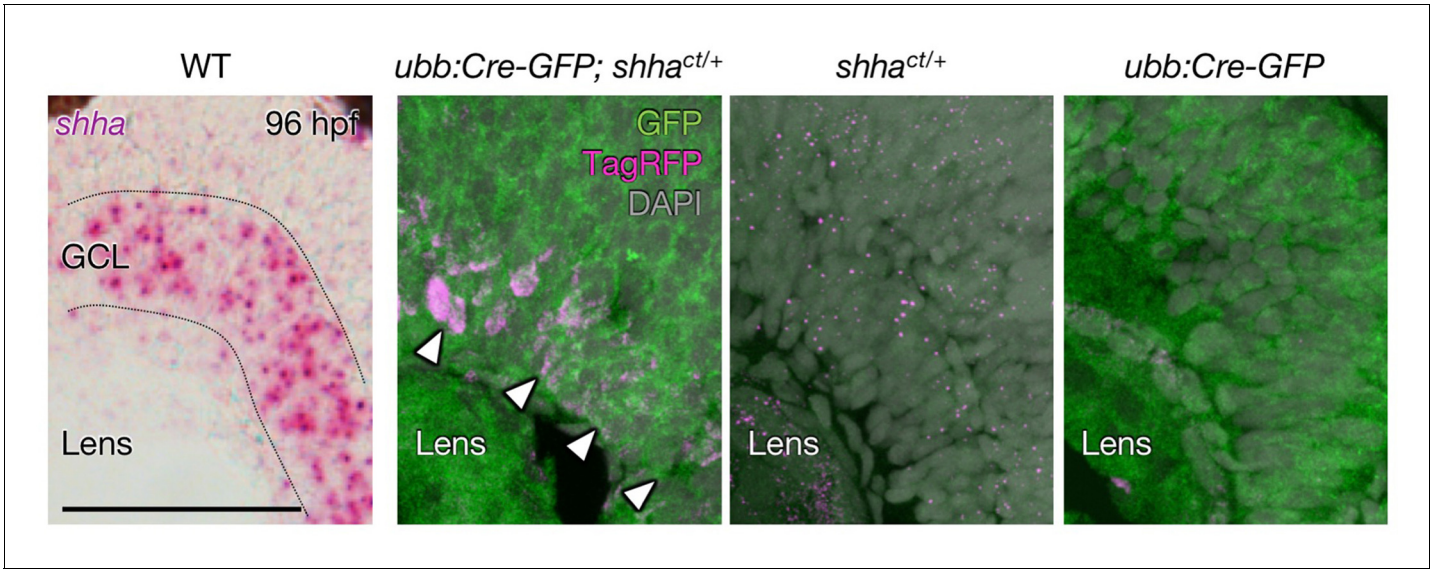

Figure 2—figure supplement 3. TagRFP expression from the inverted *shha*^{ct} allele. Weak expression of TagRFP was detected in cells in the ganglion cell layer (GCL) in the retina of *ubb:Cre-GFP; shha*$^{ct/+}$ embryos but not in *shha*$^{ct/+}$ and *ubb:Cre-GFP* embryos. Confocal projections of z-stacks are shown in three panels from the right, and the bright field image of in situ hybridization of *shha* mRNA is shown in the far left panel. Dotted lines, approximate border of the GCL. Scale bar, 50 μm.

DOI: 10.7554/eLife.24635.008

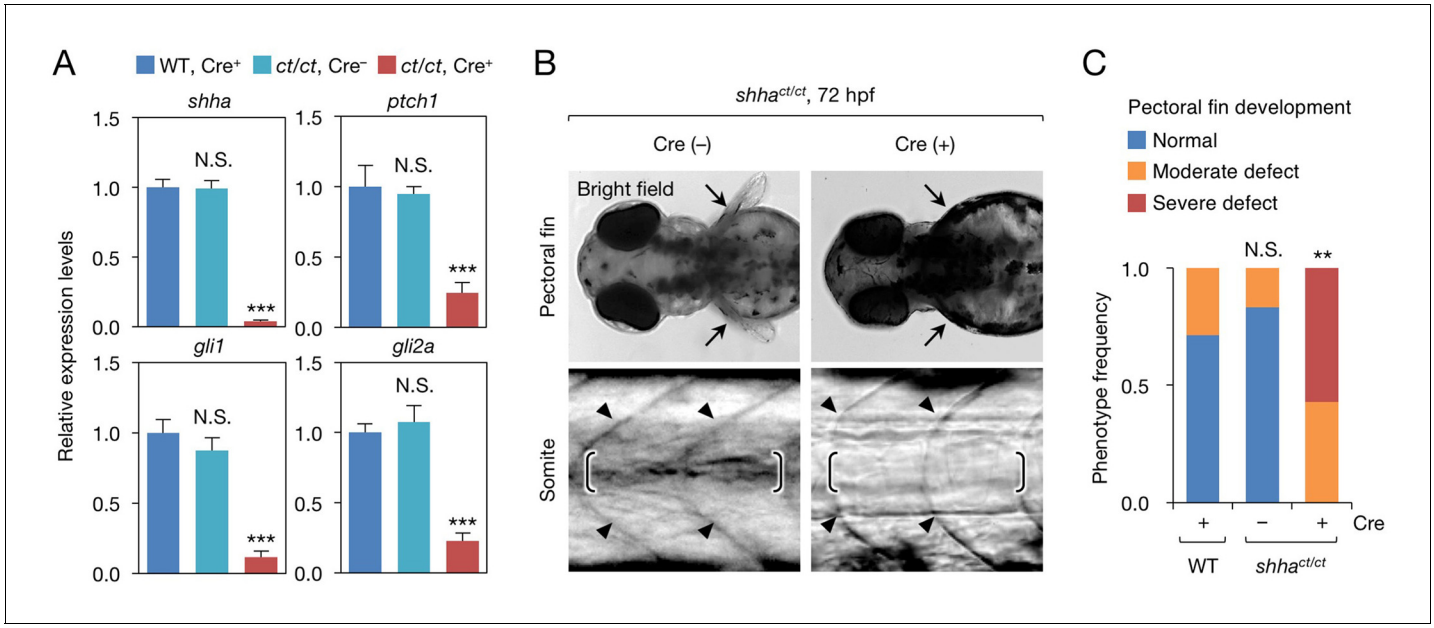

Figure 3. Phenotype of *shha*$^{ct/ct}$ embryos globally expressing Cre. (**A**) qRT-PCR analysis of 72 hpf Cre^{+} and Cre^{-} *shha*$^{ct/ct}$ embryos (n = 10 and 9). WT embryos injected with pUbb-iCRE-GFP DNA were used as a control (n = 9). Ten pooled embryos per sample were used for qRT-PCR analysis. The data are presented as the mean ± SEM (***p<0.001, Mann–Whitney U test). (**B**) Phenotypes of 72 hpf Cre^{+} and Cre^{-} *shha*$^{ct/ct}$ embryos. Arrows, pectoral fins; arrowheads, somite boundaries; brackets, horizontal myoseptum. Bright field images were captured using an MVX10 microscope. The composite images shown were generated using ImageJ software. Somite defects were observed in all embryos with severe pectoral fin defects. (**C**) Quantification of pectoral fin phenotypes from the embryos in **B** (n = 7 [WT, Cre^{+}], n = 12 [*shha*$^{ct/ct}$, Cre^{-}], and n = 28 [*shha*$^{ct/ct}$, Cre^{+}]; **p<0.01, Fisher's exact test). N.S., not significant (p=0.5392). The embryos used in **A–C** were selected on the basis of their high-level expression of Cre as described in ***Figure 2—figure supplement 1B*** (see also Cre DNA and mRNA injection, Materials and methods). A moderate pectoral fin defect was observed in control samples, likely due to injection artifacts.

DOI: 10.7554/eLife.24635.009

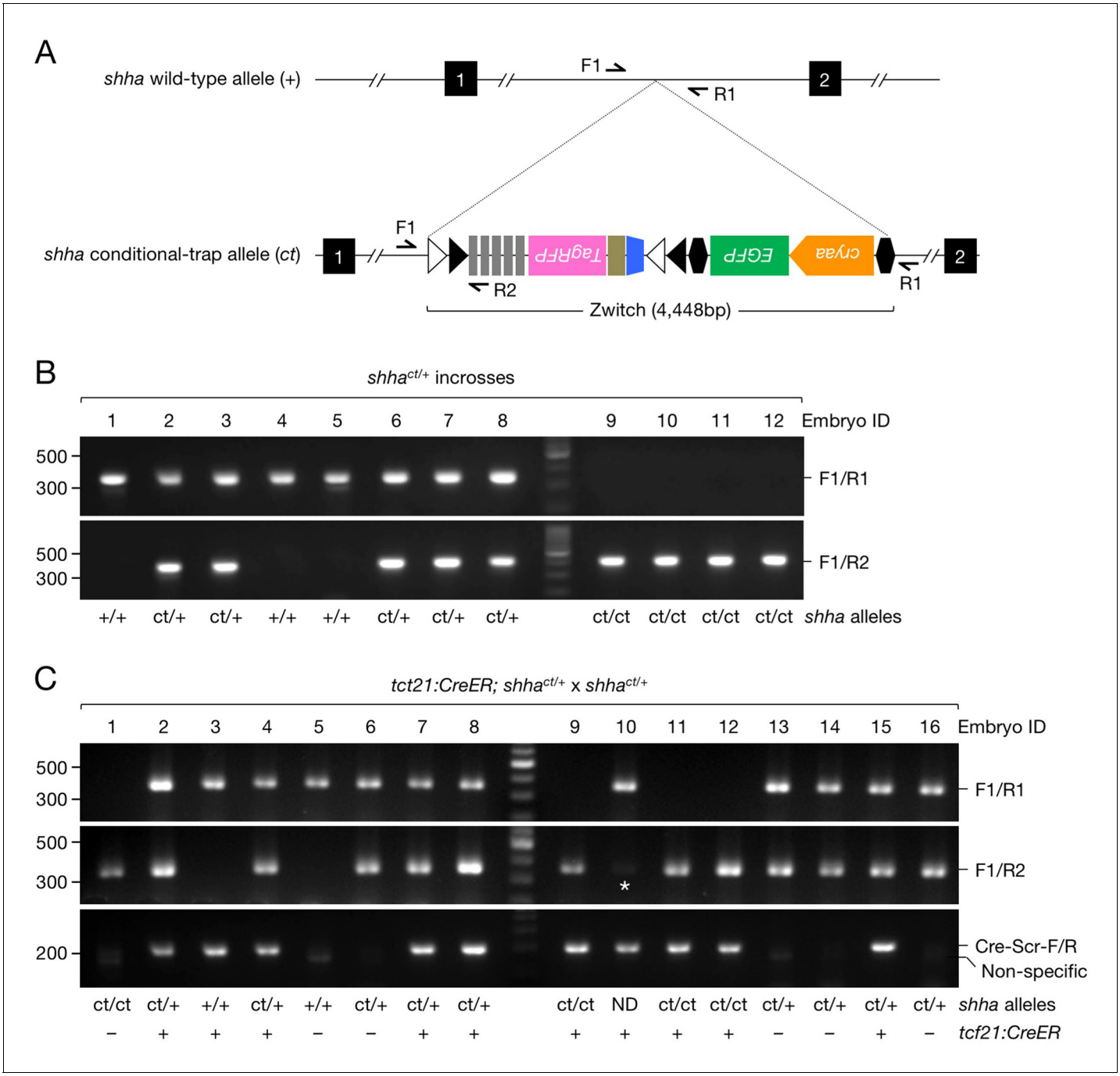

Figure 3—figure supplement 1. Genotyping PCR of *shha*^{ct} alleles. (**A**) Schematic of the *shha* WT allele (+) and conditional trap allele (*ct*) and primers sites. (**B**) Genotyping PCR result of single embryos from an incross of *shha*$^{ct/+}$ fish injected with Cre DNA at single-cell stage. Note that *ct/ct* genotype was predictable due to the developmental defects observed in *shha*$^{ct/ct}$ embryos after Cre DNA injection. (**C**) Genotyping PCR result of single embryos from a cross of *tcf21:CreER; shha*$^{ct/+}$ fish with *shha*$^{ct/+}$ fish. We did not use embryos exhibiting a faint band for experiments (asterisk). PCR with Cre-Scr-F/R primers occasionally amplified a faint non-specific band at a lower size. ND, not determined. Please see the Genotyping and Sample preparation for embryo genotyping and analysis section in the Materials and methods for details of the screening procedures.

DOI: 10.7554/eLife.24635.010

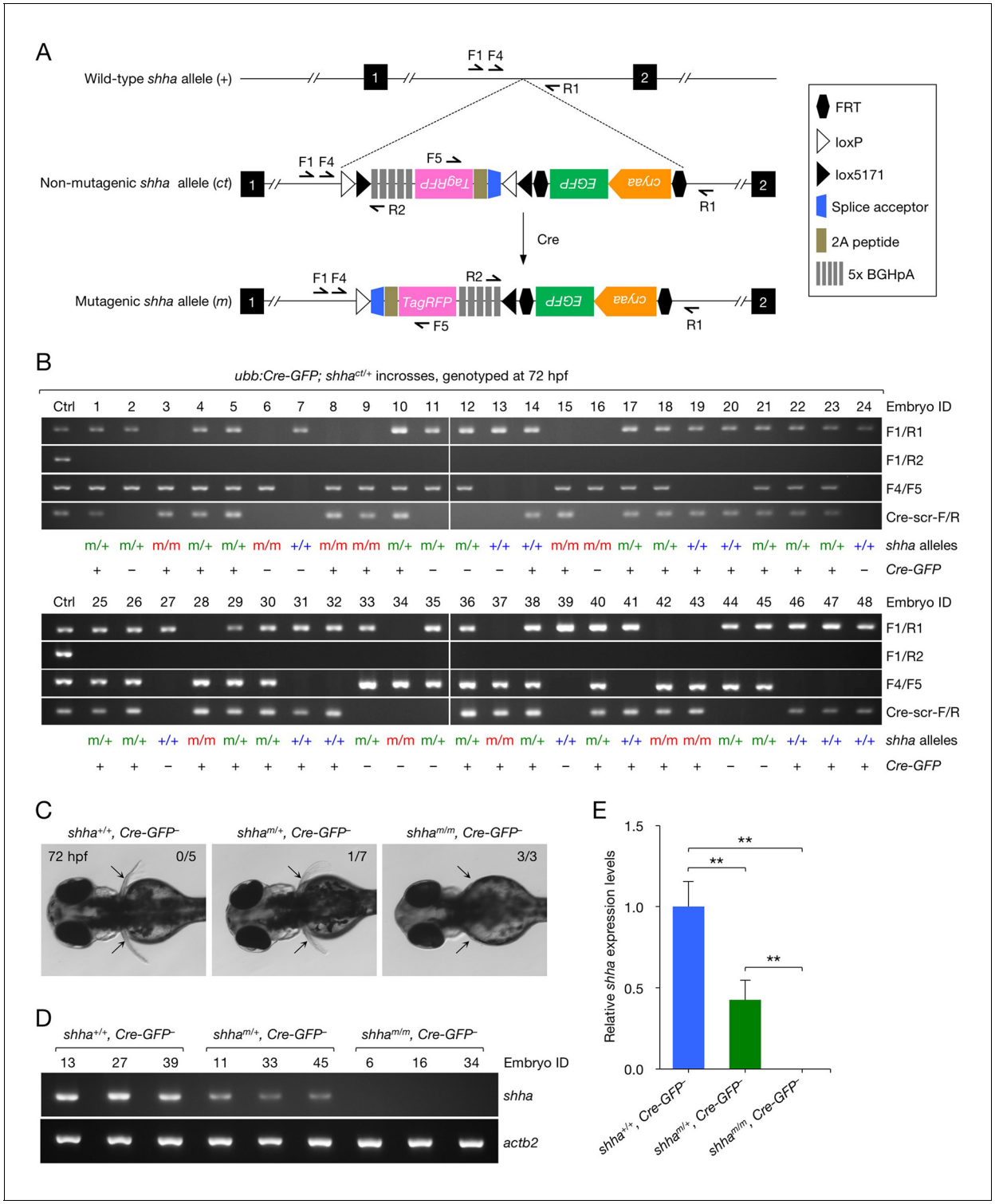

Figure 3—figure supplement 2. Analysis of embryos carrying mutagenic *shha* alleles. (**A**) Schematic of the *shha* WT allele (*+*), non-mutagenic, conditional-trap allele (*ct*), and inverted mutagenic allele (m), and primers sites. (**B**) Genotyping PCR result of single embryos from incrosses of *ubb:Cre-GFP; shha*$^{ct/+}$ fish. (**C**) Pectoral fin phenotype of WT and heterozygous and homozygous mutagenic embryos in **B**. Embryos that did not carry *ubb:Cre-GFP* transgene were analyzed (*Cre-GFP*$^{-}$). Pectoral fin development was normal in all WT embryos (0 abnormal in 5 analyzed) and most heterozygous mutants (1 moderately abnormal in 7 analyzed; p=0.3774, Fisher's exact test), but severely hampered in all homozygous mutants (3 abnormal in 3 analyzed; p<0.01, Fisher's exact test). (**D**) Semi-qRT-PCR analysis of *shha* expression in WT and heterozygous and homozygous mutagenic embryos. The

Figure 3—figure supplement 2 continued on next page

Figure 3—figure supplement 2 continued

number above each lane in the gel picture indicates the Embryo ID in **B**. (**E**) Densitometric quantification of the PCR result in **D**. The data represent the mean ± SD (**p<0.01; Mann–Whitney U test).

DOI: 10.7554/eLife.24635.011

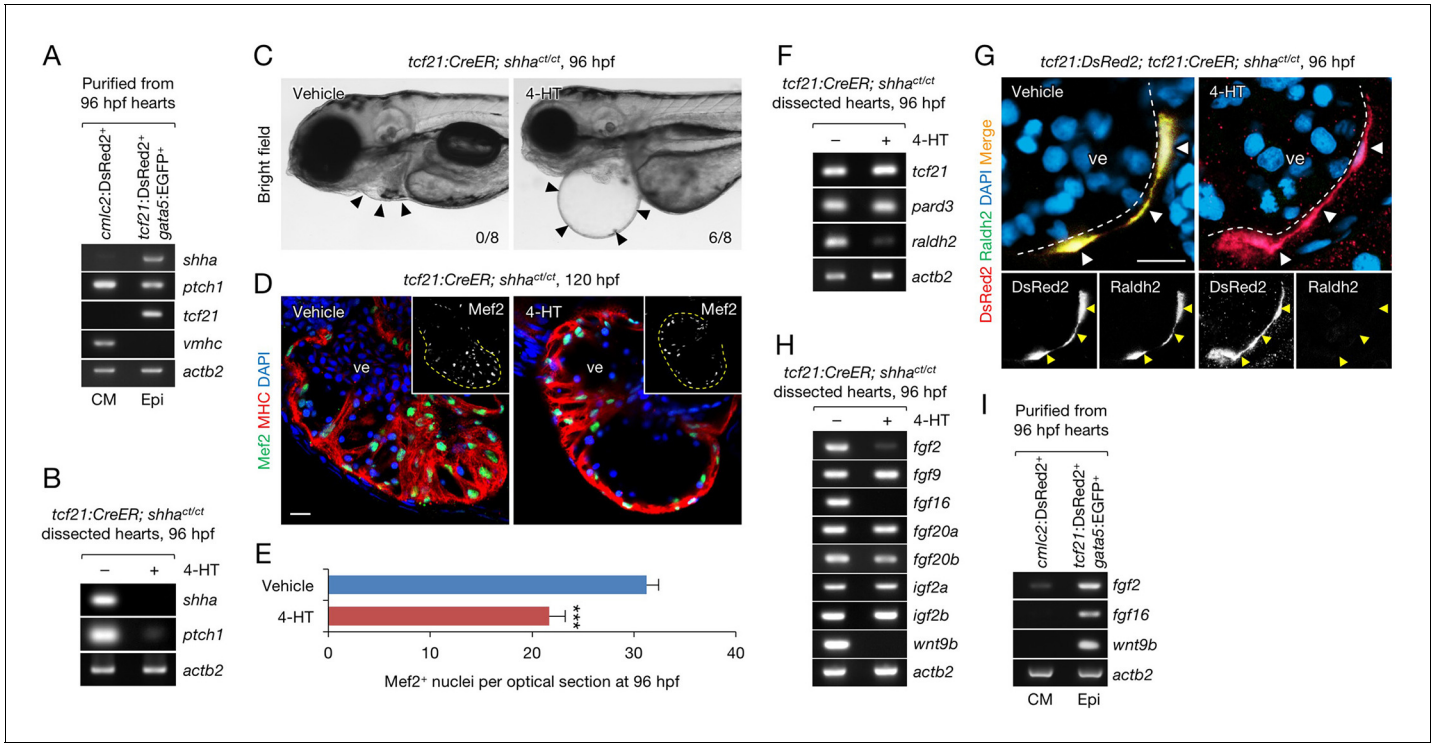

Figure 4. Epicardium-specific inactivation of *shha* expression during heart development. (**A**) Semi-qRT-PCR analysis of purified cardiomyocytes (CM) and epicardial cells (Epi) from 96 hpf hearts (see also Flow Cytometry, Materials and methods). Cardiomyocyte (*vmhc*) and epicardial (*tcf21*) markers were used to confirm the specificity of cell sorting. (**B**) Semi-qRT-PCR analysis of *shha* and *ptch1* expression in hearts dissected from *tcf21:CreER; shha*$^{ct/ct}$ embryos treated with the vehicle (–) or 4-HT (+). (**C**) Phenotype of *tcf21:CreER; shha*$^{ct/ct}$ embryos treated with the vehicle or 4-HT. Severe cardiac edema was observed in 4-HT–treated embryos at 96 hpf (six abnormal in eight analyzed; right, arrowheads) but not in vehicle-treated embryos (zero abnormal in eight analyzed; left, arrowheads; $n = 8$ each; $p<0.01$, Fisher's exact test). (**D**) Immunofluorescence of heart sections obtained from vehicle- or 4-HT–treated *tcf21:CreER; shha*$^{ct/ct}$ embryos. Insets, single-channel images of Mef2 immunofluorescence. Dotted yellow lines in insets depict the outline of the ventricle. (**E**) Quantification of Mef2^{+} nuclei from the sections obtained from the vehicle- or 4-HT–treated *tcf21:CreER; shha*$^{ct/ct}$ embryos in D ($n = 13$ and 12). The data are presented as the mean ± SEM (***$p<0.001$, Mann–Whitney U test). (**F**) Semi-qRT-PCR analysis of epicardial marker gene expression in hearts dissected from *tcf21:CreER; shha*$^{ct/ct}$ embryos treated with the vehicle (–) or 4-HT (+). (**G**) Immunofluorescence staining of heart sections obtained from vehicle- or 4-HT–treated *tcf21:CreER; shha*$^{ct/ct}$ embryos. Raldh2 immunofluorescence was detected in *tcf21*:DsRed2^{+} epicardial cells in vehicle-treated embryos (left, arrowheads) but not in 4-HT-treated embryos (right, arrowheads). Bottom panels, single-channel images of Raldh2 immunofluorescence. (**H**) Semi-qRT-PCR analysis of the expression of myocardial growth factor genes in hearts dissected from *tcf21:CreER; shha*$^{ct/ct}$ embryos treated with the vehicle (–) or 4-HT (+). (**I**) Semi-qRT-PCR analysis of *shha*-dependent myocardial growth factor genes in purified cardiomyocytes (CM) and epicardial cells (Epi) obtained from 96 hpf hearts. Single confocal sections are shown in **D** and **G**. ve, ventricle. Scale bar, 10 µm.

DOI: 10.7554/eLife.24635.012

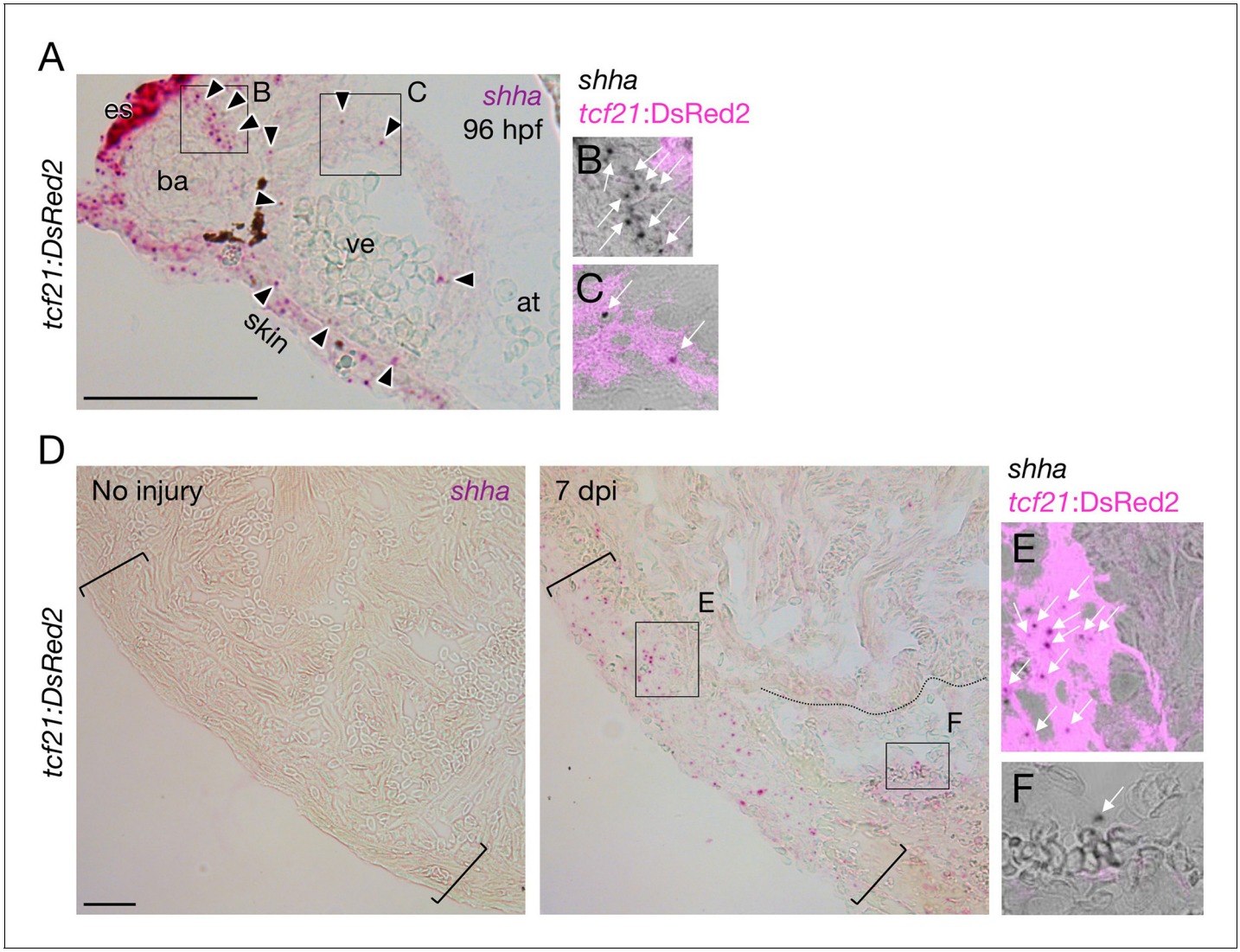

Figure 4—figure supplement 1. *shha* expression during heart development and regeneration. (**A–C**) *shha* expression during heart development in zebrafish. Single confocal slice images of the rectangles in **A** are shown in **B** and **C**. (**D–F**) *shha* expression during heart regeneration in zebrafish. Single confocal slice images of the rectangles in the right panel of **D** are shown in **E** and **F**. at, atrium; ba, bulbus arteriosus; es, esophagus; ve, ventricle. Scale bar, 50 μm.

DOI: 10.7554/eLife.24635.013

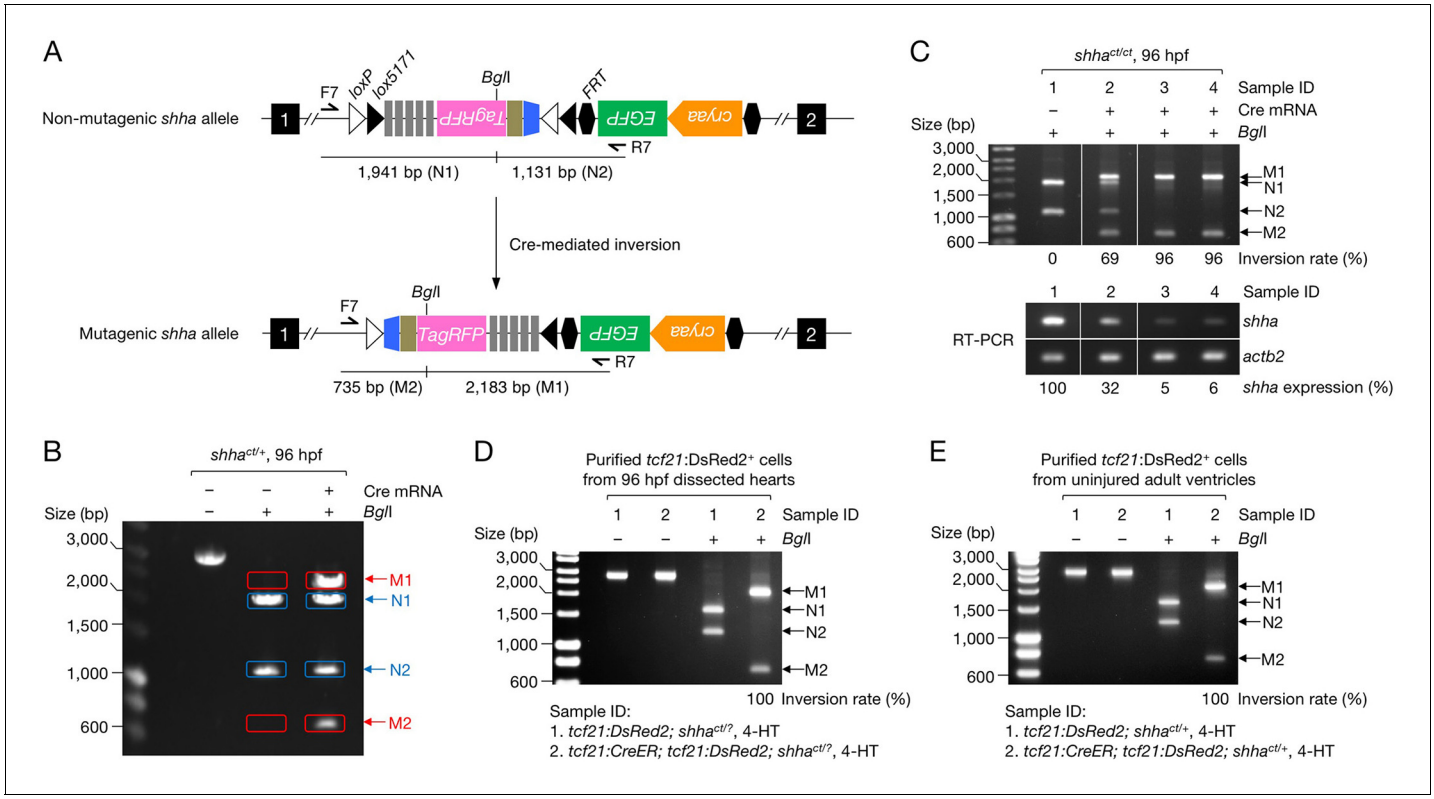

Figure 4—figure supplement 2. Inversion rate measurement. (**A**) Schematic of the non-mutagenic and mutagenic allele, primer sites, and *BglI* recognition site. (**B**) A gel image showing the PCR products of the non-mutagenic alleles without (left) and with *BglI* digestion (middle) and the PCR products of the mutagenic alleles with *BglI* digestion (right). Genomic DNA was prepared from 96 hpf *shha*$^{ct/+}$ embryos injected with (+) or without (–) Cre mRNA at single-cell stage. Cre mRNA was prepared from linearized pCS2-iCRE-BFP, in which iCRE cDNA is linked to TagBFP via P2A peptide sequence. (**C**) Analysis of inversion rate and *shha* expression levels in single embryos. Embryos were prepared from an incross of *shha*$^{ct/+}$ fish and injected with Cre mRNA at single-cell stage. Embryos without Cre mRNA injection were used as control (Sample 1). The injected embryos were separated based on the expression of TagBFP at moderate (Sample 2) and high levels (Sample 3 and 4). Individual embryos were genotyped at 96 hpf and genomic DNA and total RNA of each embryo using TRIzol following the manufactured protocol. The upper panels are the gel images used for inversion rate measurement. The numbers on the bottom are the obtained inversion rate in each sample. The lower panels are the results of semi-qRT-PCR analysis of *shha* expression levels of each sample. (**D**) Analysis of inversion rate in epicardial cells in zebrafish embryos. Embryos were prepared from crosses of *tcf21:DsRed2; shha*$^{ct/+}$ fish with *shha*$^{ct/+}$ fish (Sample 1) and *tcf21:CreER; shha*$^{ct/+}$ fish with *tcf21:DsRed2; shha*$^{ct/+}$ fish (Sample 2). Embryos were treated with 4-HT and examined for DsRed2 expression to screen *tcf21:DsRed2* transgene and lens EGFP expression to screen *tcf21:CreER* transgene (***Kikuchi et al., 2011***). Lens EGFP from *tcf21:CreER* transgene is considerably stronger than that from *shha*^{ct} alleles in embryos, which enables us to sort *tcf21:CreER*$^{+}$ embryos with *shha*^{ct} background. PCR genotyping on *shha*^{ct} alleles were not performed; this does not affect the measurement as the inversion rate is quantified based on the PCR products of the *shha*^{ct} alleles. *tcf21*:DsRed2^{+} epicardial cells were isolated by FACS and 1,000 DsRed2^{+} cells were used for analysis. The estimated inversion rate is 100%; note that the bands from the non-mutagenic allele (N1 and N2) are undetectable in Sample 2 after *BglI* digestion. (**E**) Analysis of inversion rate in epicardial cells in the adult zebrafish ventricle. Ventricles were prepared from 4-HT–treated adult *tcf21:DsRed2; shha*$^{ct/+}$ fish (Sample 1) and *tcf21:CreER; tcf21:DsRed2; shha*$^{ct/+}$ fish (Sample 2). *tcf21*:DsRed2^{+} epicardial cells were isolated by FACS and 5000 DsRed2^{+} cells were used for analysis. The estimated inversion rate is 100%; note that the bands from the non-mutagenic allele (N1 and N2) are undetectable in Sample 2 after *BglI* digestion.

DOI: 10.7554/eLife.24635.014

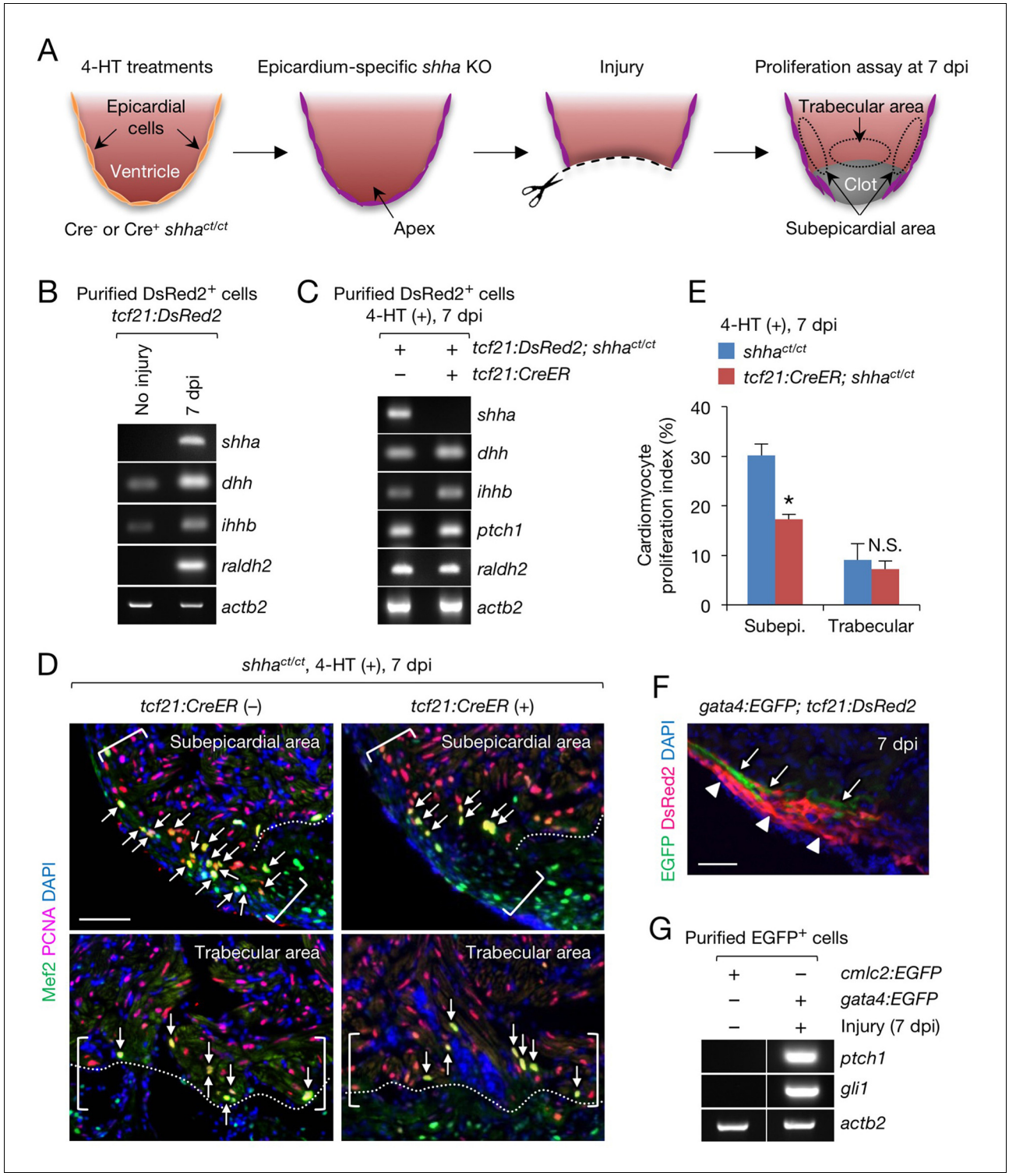

Figure 5. Epicardial *shha* expression promotes subepicardial cardiomyocyte proliferation during heart regeneration. (**A**) Schematic of the experiment. (**B**) Semi-qRT-PCR analysis of *shha* in purified *tcf21*:DsRed2^{+} epicardial cells obtained from uninjured and injured (7 dpi) *tcf21*:DsRed hearts. Injury was confirmed by the induction of *raldh2* expression. (**C**) Semi-qRT-PCR analysis of Hh pathway genes using purified *tcf21*:DsRed2^{+} epicardial cells obtained from 4-HT–treated 7 dpi *tcf21:DsRed; shha*$^{ct/ct}$ (control, left) and *tcf21:DsRed; tcf21:CreER; shha*$^{ct/ct}$ hearts (right). (**D**) Immunofluorescence images of the subepicardial (top) and trabecular areas (bottom) of heart sections obtained from 4-HT–treated 7 dpi *shha*$^{ct/ct}$ (control) or *tcf21:CreER; shha*$^{ct/ct}$ hearts. Brackets, subepicardial areas. Dotted lines, approximate amputation plane. Arrows indicate proliferating cardiomyocytes. (**E**) Quantification of cardiomyocyte proliferation in the subepicardial and trabecular areas of the heart sections obtained from 4-HT–treated 7 dpi *shha*$^{ct/ct}$ (control) or *tcf21:*

Figure 5 continued on next page

Figure 5 continued

CreER; shha$^{ct/ct}$ hearts shown in D (n = 6 each). The data are presented as the mean ± SEM (**p<0.01, Mann–Whitney U test). N.S., not significant (p=0.3367). (**F**) Image of heart sections obtained from 7 dpi *gata4:EGFP; tcf21;DsRed2* fish. Subepicardial cardiomyocytes (green, arrows) associate with epicardial cells (magenta, arrowheads). (**G**) Semi-qRT-PCR analysis of *shha* pathway genes using purified subepicardial cardiomyocytes obtained from 7 dpi *gata4:EGFP* ventricles. Cardiomyocytes purified from uninjured *cmlc2:EGFP* ventricles were used as negative controls. Scale bar, 50 μm.

DOI: 10.7554/eLife.24635.015

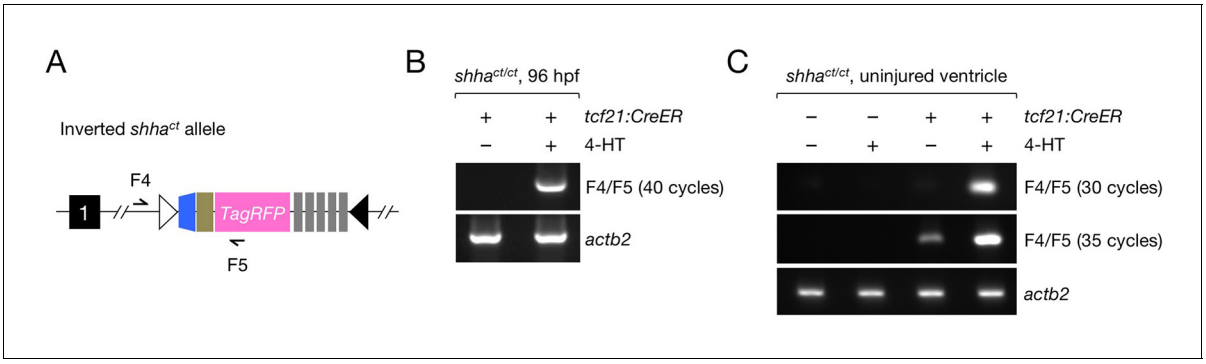

Figure 5—figure supplement 1. Assessment of spontaneous cassette inversion. (**A**) Schematic of the inverted *shha*^{ct} allele and primers sites. (**B**) The inverted allele was not detected in untreated *tcf21:CreER; shha*$^{ct/ct}$ embryos using 40 cycles of PCR. (**C**) The inverted allele was not detected in untreated adult *tcf21:CreER; shha*$^{ct/ct}$ fish using 30 cycles of PCR, but it was detected when the cycle number was increased to 35. Each PCR sample used genomic DNA isolated from five pooled hearts as a template.

DOI: 10.7554/eLife.24635.016

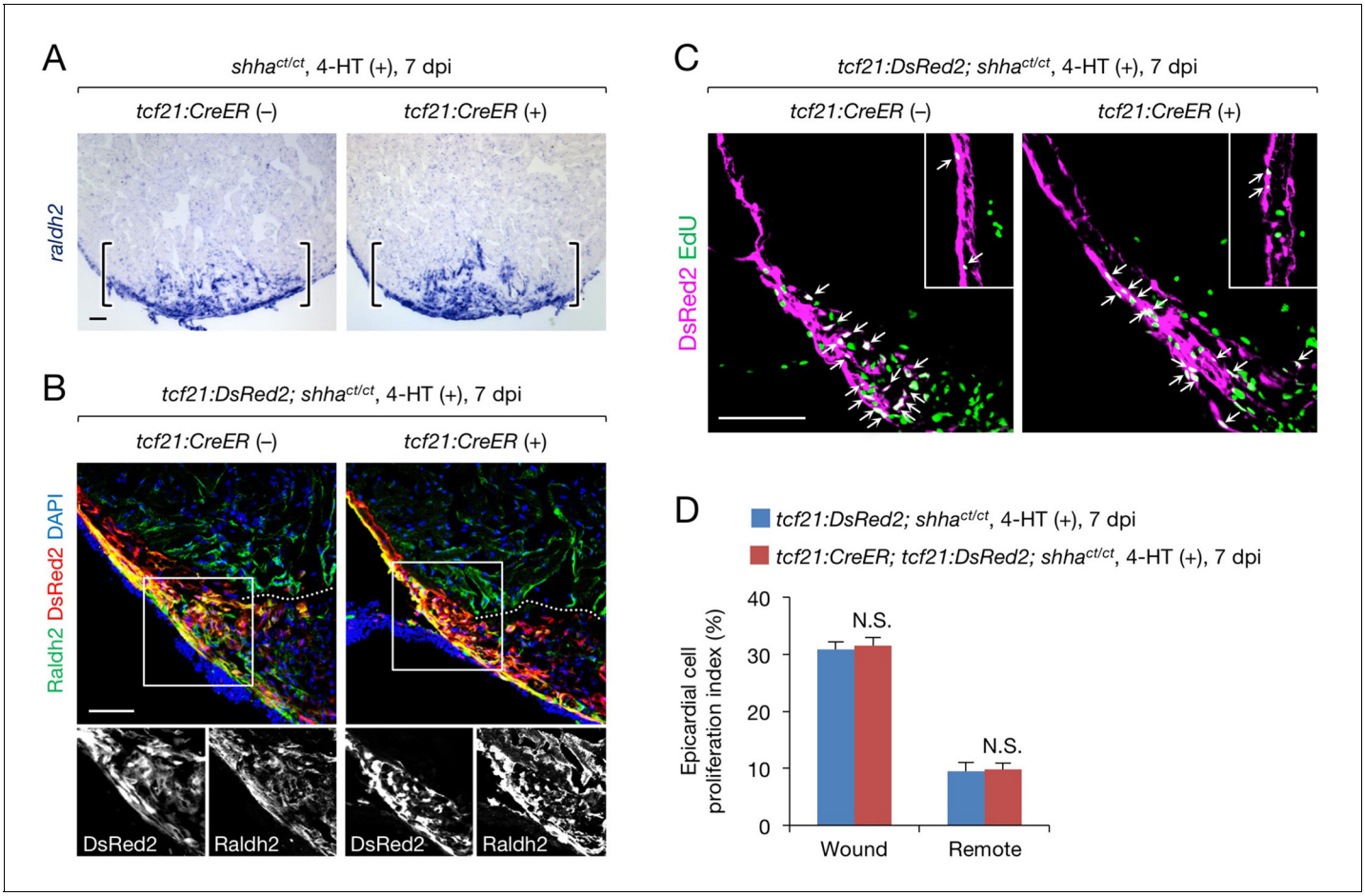

Figure 5—figure supplement 2. A redundant role for epicardial *shha* in epicardial migration and proliferation during heart regeneration. (**A**) In situ hybridization analysis of *raldh2* expression in sections obtained from 4-HT-treated 7 dpi *shha*$^{ct/ct}$ (control) and *tcf21:CreER; shha*$^{ct/ct}$ hearts. Brackets, injury site. (**B**) Immunofluorescence staining of Raldh2 and DsRed2 using sections obtained from 4-HT-treated 7 dpi *tcf21:DsRed; shha*$^{ct/ct}$ (control) and *tcf21:DsRed; tcf21:CreER; shha*$^{ct/ct}$ hearts (right). Single-channel images of the rectangle are shown at the bottom. Dotted line, approximate amputation plane. (**C**) Immunofluorescence staining of DsRed2 and EdU in sections obtained from 4-HT-treated 7 dpi *tcf21:DsRed; shha*$^{ct/ct}$ (control) and *tcf21:CreER; tcf21:DsRed; shha*$^{ct/ct}$ hearts. Inset, non-injured area. Arrows indicate proliferating *tcf21*$^{+}$ epicardial cells, which were defined as epicardial cells colabeled DsRed2 and EdU. (**D**) Quantification of epicardial cell proliferation in the sections obtained from 4-HT-treated 7 dpi *tcf21:DsRed; shha*$^{ct/ct}$ (control) and *tcf21:CreER; tcf21:DsRed; shha*$^{ct/ct}$ hearts shown in **C** (n = 5 each). The data represent the mean ± SEM (wound, p=0.754; remote, p=0.602; Mann–Whitney U test). N.S., not significant. Single confocal slice images are shown in **B** and **C**. Scale bar, 50 μm.

DOI: 10.7554/eLife.24635.017